TITLE: Use of RANS Calculations in the Design of a Submarine Sail

DISTRIBUTION: Approved for public release, distribution unlimited
Availability: Hard copy only.

This paper is part of the following report:

TITLE: Reduction of Military Vehicle Acquisition Time and Cost through
Advanced Modelling and Virtual Simulation [La reduction des couts et des
delais d'acquisition des vehicules militaires par la modelisation avancee et
la simulation de produit virtuel]

To order the complete compilation report, use: ADA415759

The component part is provided here to allow users access to individually authored sections
of proceedings, annals, symposia, etc. However, the component should be considered within
the context of the overall compilation report and not as a stand-alone technical report.

The following component part numbers comprise the compilation report:
ADP014142 thru ADP014198

# Use of RANS Calculations in the Design of a Submarine Sail

**Joseph J. Gorski and Roderick M. Coleman**
NSWC, Carderock
9500 MacArthur Boulevard
West Bethesda, MD 20817-5700, USA

## Abstract

The application of a Reynolds Averaged Navier-Stokes (RANS) code in the design of an "Advanced Sail" for a submarine is discussed. To validate the code on similar sail shapes calculations are compared with experimentally obtained data at 1/35 scale from a wind tunnel and 1/17 scale from a water channel. This data comparison includes flow visualization, axial velocity and surface pressures. The agreement demonstrates that RANS codes can be used to provide the significant hydrodynamics associated with these sail shapes. To improve the design several modifications to a sail are evaluated using the RANS code. Based on the predicted secondary flow downstream of the sail as well as the drag a new design is chosen, without having to build and test the inferior shapes, reducing time and cost for the program. This improved sail was then built at 1/4 scale and demonstrated on the U.S. Navy's Large Scale Vehicle.

## Introduction

The U. S. Navy is investigating the benefits of an "Advanced Sail" for improved effectiveness in littoral regions while minimizing the impact on performing traditional missions. The canopy-like shapes, Fig. 1, provide a significant increase in payload over conventional sails. The increased volume, on the order of a factor of four over conventional airfoil shaped sails, can be used for special operating forces stowage, high data rate antennae, countermeasures, littoral warfare missiles, and other payload systems while maintaining all current systems and capabilities, Dozier et al [1]. To minimize impact the Advanced Sail designs cannot significantly add to the drag of the submarine or degrade the flow into the propeller over conventional designs, despite the increased size.
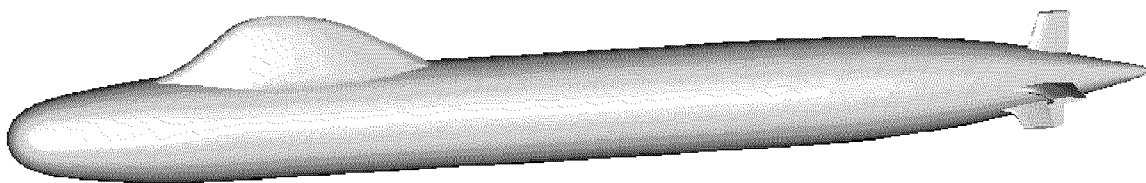


Fig. 1 Submarine configured with an Advanced Sail.

Submarines are basically axisymmetric bodies with appendages to offer a minimum of resistance so that the vehicles can be economically powered and move efficiently through the water. Appendages provide an opportunity for wakes and vortices to be generated which can impact drag and quiet operation of a submarine, which are critical in its design. Any protrusions from the surface will tend to increase the drag, due to pressure gradients, increased wetted surface area, and energy spent in vortex generation. Vortices typically consist of necklace vortices from hull/appendage junctions, tip vortices from the appendages, and vortices generated directly from the hull due to angles of attack. The vortical flow generated from the hull and appendages can also significantly influence the maneuvering characteristics of a submarine. Spatial flow

distortions into the propeller created by upstream wakes, vortices or flow separations can contribute to noise generation as well as propeller vibration. The largest appendage on any submarine is usually the sail and consequently its drag and wake are important considerations in a design. Increasing its size by a factor of four over conventional sails, while minimizing impact on drag or propeller inflow, requires streamlined shapes due to the much larger wetted surface area. Additionally, longitudinal vortices are created downstream of canopy sails, such as these, even with their streamlined shapes, Gorski [2]. To minimize these secondary flows, as well as the drag, created by these large sails requires a large amount of building and testing of models or computations of candidate shapes for evaluation.

To reduce schedule and cost the Advanced Sail program has relied heavily on computational fluid dynamics (CFD) tools to help in the hydrodynamic evaluation of the sail shapes. The main hydrodynamic considerations for the Advanced Sail shapes are minimizing drag and secondary flow created by them. Because of the viscous nature of these areas inviscid calculations are of limited value and Reynolds Averaged Navier-Stokes (RANS) codes have been the focus of the computational effort. Perhaps the first fully appended submarine RANS calculation was done by Gorski et al [3] for the SUBOFF configuration, which was extensively measured [4] to provide a data-base to test CFD methods. At the time of the SUBOFF program it was shown that RANS calculations could predict the pressures quite well and some of the mean flow, but generally under predicted the strength of necklace vortices. Since that time there have been considerable efforts directed at submarine RANS calculations, Gorski [2]. Modern RANS codes take advantage of the large parallel computers and provide calculations on much finer grids than at the time of SUBOFF. This allows for better flow predictions, in a timely manner, and RANS codes are accurate enough and have matured to a point where they can be used for submarine design [5].

In general a new paradigm for surface ship and submarine design is evolving which uses a mix of experiments and computations. The days of the old series tests, where systematic variations of a hull form are built and tested experimentally, are fading due to time and cost considerations and since computations are an attractive alternative. In particular, viscous calculations are becoming faster and more affordable as gridding improves and computers get more powerful. However, confidence needs to be built up in the predictions. Despite the successes of RANS predicting drag and detailed flow into the propeller may still be an issue, depending on how much detail is needed. Consequently, model tests are often done to provide conventional data for hull form evaluation as well as validation data for the computations. The current program involves experiments on a variety of sail shapes including: 1/35 scale models in a wind tunnel, 1/17 scale models in a water channel, and a 1/4 scale demonstration. The experiments can often run through a variety of speeds and operating conditions once a model is built for shape evaluations. The computations provide a fast means to evaluate shape alternatives for sail redesign. Thus, less model construction and testing is required of shapes that can be rejected based on the computations. As more confidence is gained in the computations it may be possible to reduce model construction and testing to the final shape or shapes. The current paper demonstrates how the RANS calculations compared with some of the experimental data as well as how RANS computations are used in the redesign process for the Advanced Sail.

**CFD Process**

It should be pointed out that to perform good flow calculations is not simply a matter of turning on a particular piece of software, particularly for complicated geometries or flows. The computations, with either RANS or potential flow solvers, involve a process not completely unlike that of doing a model experiment. A test of whether a particular code can predict certain measured physics is dependent on all pieces of this process. An idea of what this process is like is shown in Fig. 2. The validation of the calculation against experimental data depends on all of the steps in the process. A problem with any one of them can lead to differences in the computed and measured data.

Prerequisite to generating computational grids is the satisfactory specification of the actual geometry. Details, such as ensuring there are no gaps in the geometry and trimming surfaces, must be taken care of before the geometry can be used easily with grid generation software. For the actual definition of the geometry, a single B-spline surface for each component is preferred. B-splines can model the most complex

shapes and provide smooth, continuous definition with well-behaved intersections. In the IGES format, they can be transferred between most CAD and grid generation software packages.
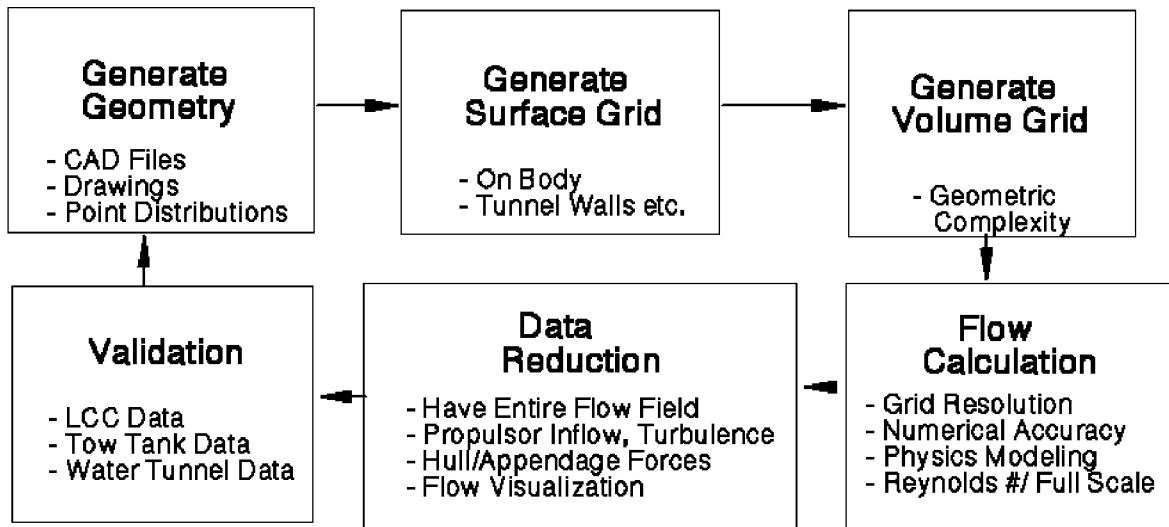
| Generate Geometry<br><br>- CAD Files<br>- Drawings<br>- Point Distributions | → | Generate Surface Grid<br><br>- On Body<br>- Tunnel Walls etc. | → | Generate Volume Grid<br><br>- Geometric Complexity |
|---|---|---|---|---|
| Validation<br><br>- LCC Data<br>- Tow Tank Data<br>- Water Tunnel Data | ← | Data Reduction<br><br>- Have Entire Flow Field<br>- Propulsor Inflow, Turbulence<br>- Hull/Appendage Forces<br>- Flow Visualization | ← | Flow Calculation<br><br>- Grid Resolution<br>- Numerical Accuracy<br>- Physics Modeling<br>- Reynolds #/ Full Scale |

Fig. 2 CFD Process

When generating the computational grid, a surface grid must first be generated on the body and all surrounding boundaries where boundary conditions are imposed. This surface grid breaks up the smooth B-spline surface into discrete points and one must make sure the grid conforms to the actual geometry. Additionally, these surface grids must be clustered in areas of high geometry gradients or where the flow is expected to change rapidly to help provide accurate predictions. It is very important in shaping or sculpting a geometry that enough attention to detail is done so that changes in the actual geometry are properly represented in the discretized geometry. A volume grid is next generated providing discrete points in the entire flow domain where the Navier-Stokes equations are solved. A computed solution can only be as good as the grid on which it is computed. If there are high gradients in the flow, such as in boundary layers, wakes and vortices, it is necessary to have enough grid points in these areas to resolve them. If enough grid points are not present the computation will diffuse these high gradients. Once a flow feature is diffused in this, or any other way, its impact and interaction on the surrounding and downstream flow cannot be predicted accurately. For viscous calculations, and drag comparisons in particular (Gorski [6]) attention must be paid to these details to insure one is predicting flow differences due to actual geometry changes and not differences due to computational changes. In practice it is sometimes difficult to achieve good grid quality, a sensible amount of time spent, and a practical grid size all at the same time. For the current computations which consist of the sail and bare hull approximately 1.2 million points are used for half the body with port/starboard symmetry assumed. With these streamlined sails, it is possible to have the grid conform to the overall surface much like a bump as shown in Fig. 3. Here 191 points are along the length of the body, 65 extend outward away from the hull and 97 wrap around it with some clustering toward the top for better sail wake definition. In the design cycle a new grid could often be generated in a few hours to days depending on the extent of the modifications.

Obviously flow solutions also depend on the RANS code used. In the current effort the incompressible Reynolds Averaged Navier-Stokes equations are solved using the Mississippi State University code UNCLE [7,8]. The equations are solved using the pseudo-compressibility approach of Chorin[9] where an artificial time term is added to the continuity equation and all of the equations are marched in this artificial time to convergence. Only steady state computations are performed for this effort. For the present calculations a third-order upwind biased discretization, based on the MUSCL approach of Van Leer et al [10], is used for the convective terms. The equations are solved implicitly using a discretized Newton-relaxation method[11] with multigrid techniques implemented for faster convergence[12]. An important factor in being able to compute and evaluate the hull modifications and operating conditions of interest is the implementation of a parallel version of the UNCLE code[13]. The code uses MPI for message passing due to its portability.

To run in parallel the computational grid is decomposed into various blocks, which are sent to different processors. Load balancing is obtained by making the blocks as equally sized as possible. For the present calculations 18 processors are used which allowed for new solutions in a few days depending on computer load. More details of the solver can be found in the various references provided.
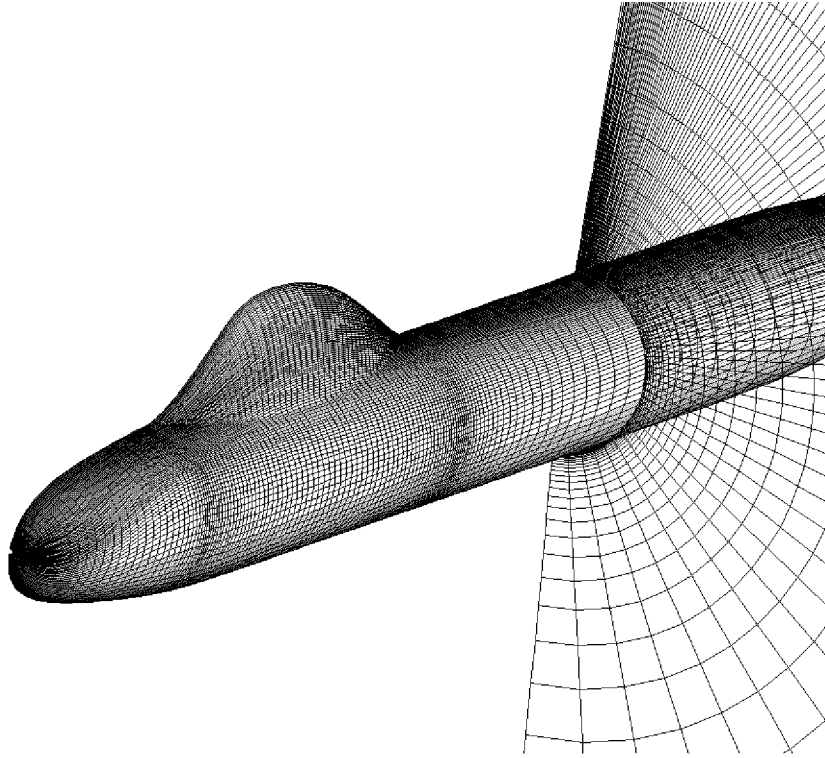


Fig. 3 Computational grid on the surface and at a single axial plane.

Another issue affecting accuracy is the turbulence modeling used. Two-equation models have become the standard for practical applications. In the current study both a $k$ - $\varepsilon$ and $q$ - $\omega$ model are used. The $k$ - $\varepsilon$ model is that developed by Liou and Shih [14] which is a variant of the model developed by Shih and Lumley [15]. The variation from the original model is the inclusion of a variable $C\mu$ based on the mean strain rate. This is a low Reynolds $k$ - $\varepsilon$ model in the sense that the equations are solved right to the wall without the use of wall functions for the mean flow. The $q$-$\omega$ model used is that developed by Coakley [16]. With this two-equation model, $q$, which is the square root of kinetic energy, is solved for rather than kinetic energy. Also, rather than solving for the rate of dissipation of turbulent kinetic energy, $\varepsilon$, here the specific dissipation rate of kinetic energy, $\omega$, is solved for. The two dissipations are related through the relation $\omega = \varepsilon/k$. One advantage of the $\omega$ formulation is that it replaces the $\varepsilon^2/k$ source term of the $\varepsilon$ equation, which is problematic near walls and other locations where kinetic energy approaches zero, with a better behaved term which adds to stability of the solution. The $q$-$\omega$ equations are also solved directly to the wall with $q$ and the normal derivative of $\omega$ both set to zero. For solving directly to the wall it is generally preferable to have the first point off of the wall well within the viscous sub-layer and a value of $y^+$ around 1 is used here. Going to higher Reynolds numbers requires the relative distance of the first point off of the wall to become smaller.

## Validation Effort

The computed solutions cover the entire flow field, whereas experimental data is available only at specific locations. Consequently, computations can provide much information not available in an experiment. To gain confidence in the calculations, particularly when doing unconventional hull forms, it is desirable to have some experimental data to validate the computations. For the Advanced Sail effort extensive

measurements have been obtained, both for design evaluation and code validation efforts. Models of several sails at 1/35 scale were tested in the Subsonic Wind Tunnel at the Naval Surface Warfare Center, Carderock Division (NSWCCD). Measurements consisted of forces and moments, surface pressures, wake surveys and flow visualization. This provided some data for code validation as well as information to help down select to two sail shapes. Models for these two candidate shapes were built, at 1/17-scale, and tested in the Navy's Large Cavitation Channel (LCC) in Memphis, TN. Measurements consisted of wake surveys and pressure measurements. To some extent this involved the traditional build and test philosophy of old although computations were used extensively to down select to the shapes tested in the wind tunnel from a large group of candidate sail shapes. However, the calculations were further used to refine the selected sail shape to a final design, which will be discussed in the redesign effort. RANS calculations have been performed on several of the wind tunnel tested models, but only the two sails also tested in the LCC are shown here.

The first sail shown here is the canopy shape of Fig. 1. Computed surface streamlines over the sail are shown in Fig. 4 and those on the hull around the sail in Fig. 5. Also shown are oil paint dot flow visualizations from the wind tunnel test, which the computations agree well with. The flow goes smoothly over and around the streamlined sail without any necklace vortex being formed. However, as discussed by Gorski [2], longitudinal vortices are still formed downstream of the sail as seen in Fig. 6, which shows secondary flow streamlines at two locations downstream of the sail. This pressure driven secondary flow, also referred to as secondary flow due to curvature, is a result of the flow turning around the sail. Transverse vorticity is generated in the hull boundary layer as the boundary layer on the hull approaches the sail. As the flow streamlines curve around the sail a longitudinal component of vorticity develops which flows downstream around the sail producing a pair of vortices similar to the necklace vortex of a wing/body junction. Although no necklace vortex is formed the large turning of the flow around the sail can lead to strong secondary flows. Enhancing this pressure driven secondary flow is flow down the back of the sail which has a component inward which impinges on the hull and can produce vortical flow of the same sense as that generated from turning around the sail. A similar effect was documented by Walter and Patel [17] for a surface mounted ellipsoid which had a very weak necklace vortex, but a strong spanwise component of flow from the tip inward to the wall at the trailing edge of the ellipsoid creating longitudinal vortices similar to a necklace vortex. This overall secondary flow causes the streamlines behind the sail to move outward away from the centerline, Fig. 5. Laser Doppler Velocimetry (LDV) measurements were obtained in the LCC at various axial locations. Shown in Fig. 7 is the measured axial velocity at X/L = 0.825 as compared to the calculations with both turbulence models. There is a significant bulge in the axial velocity due to the longitudinal vortices, which convect high velocity flow in toward the hull along the centerline and low velocity boundary layer flow away from the hull outboard from the centerline. The k - ε prediction has smoothed out the bulge considerably where as the q - ω model predicts it nicely. To insure this is a turbulence modeling issue a finer grid was also run with 129 points wrapping around ½ the body and more clustering toward the centerline, but the finer grid provided little difference in the predicted flow field. This shows the k - ε model is damping out the vortex too much, which is not unusual for the k - ε model in general, Gorski [18]. Computed and measure surface pressures on the sail are shown in Fig. 8.
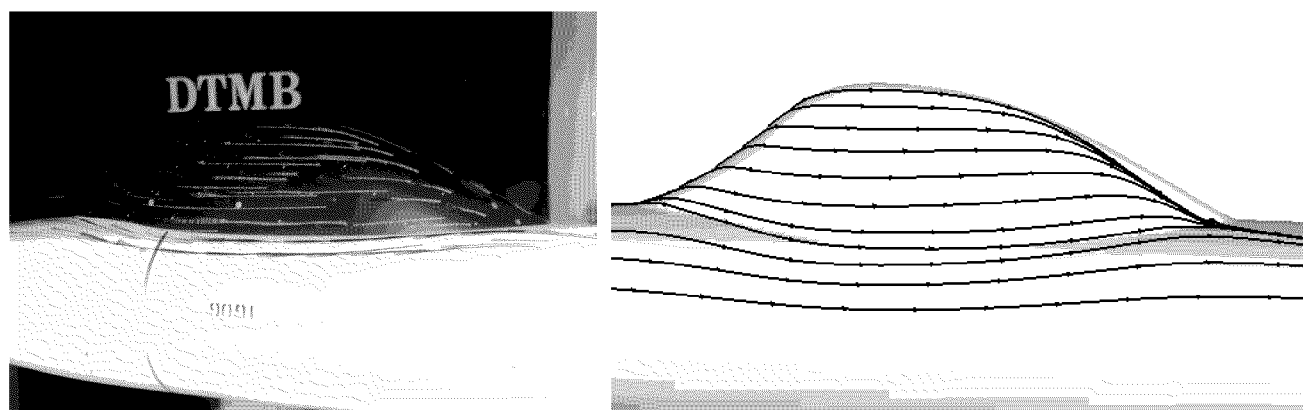


Fig. 4 Wind tunnel oil flow traces and computed surface streamlines for canopy sail.
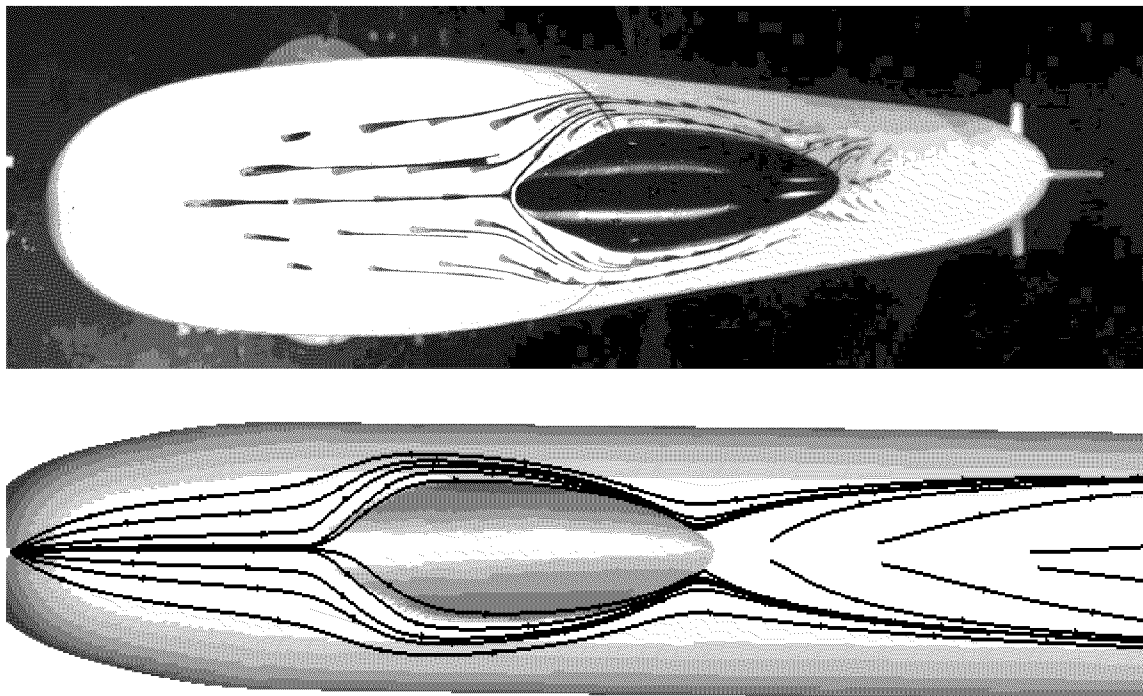
Fig. 5  Wind tunnel oil flow traces and computed surface streamlines around the canopy sail.
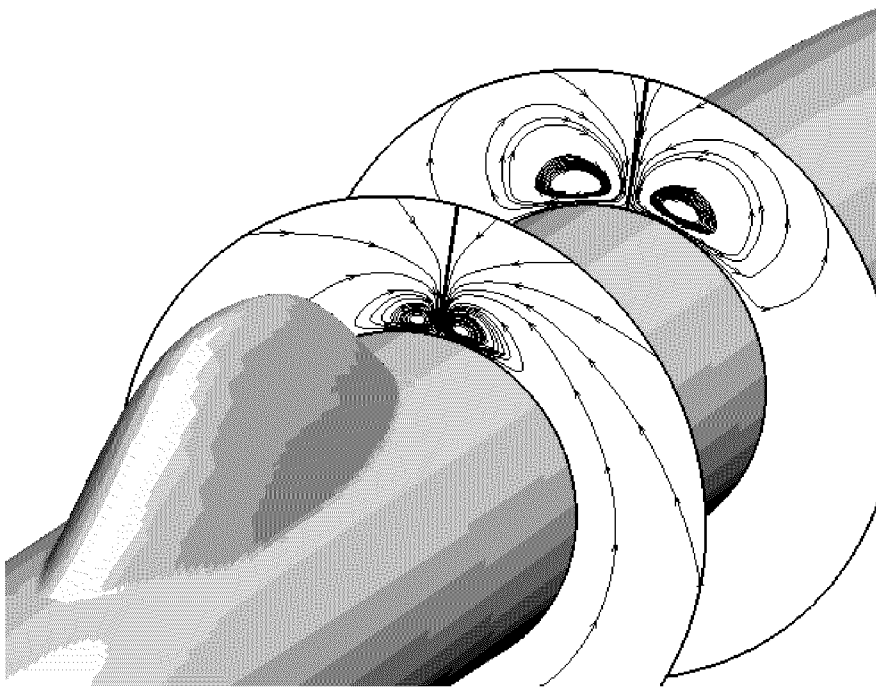


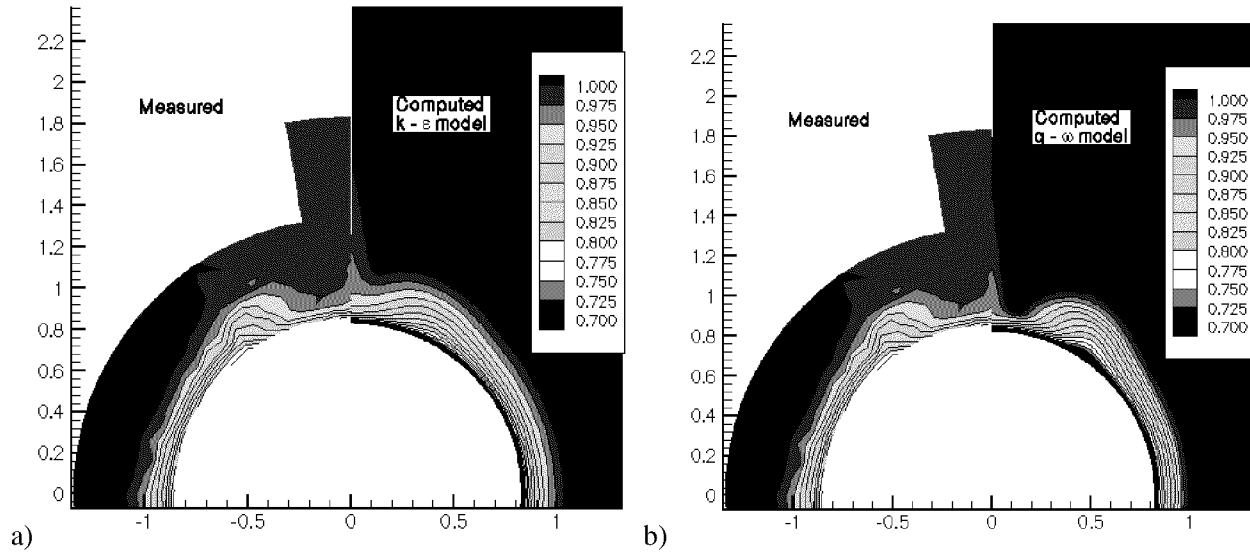Fig. 6  Secondary flow streamlines downstream of the sail.

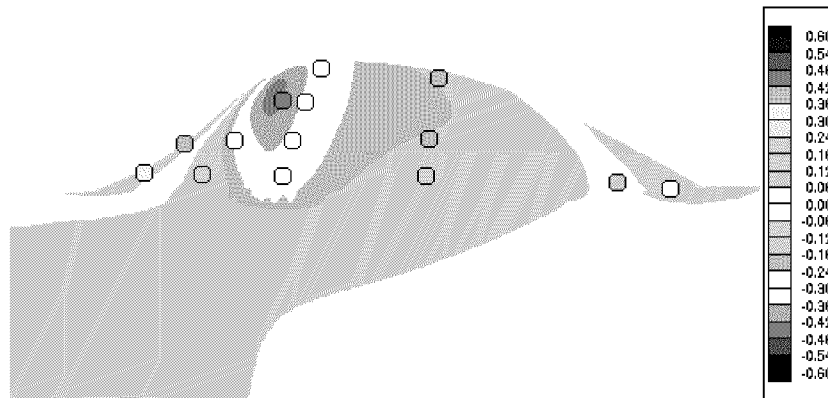Fig. 7 Comparison of measured and computed axial velocity at X/L = 0.825 a) k-ε model b) q-ω model.



Fig. 8 Cp on the sail as compared with LCC measured values.

A second shape tested in the LCC is considerably different than the first. The height of this second shape rises more quickly than the first, but still has a large fillet at the leading edge. It is rounded over the top and has a rather blunt trailing edge, which probably is what leads to greater drag for this configuration than the first. The flow goes smoothly around the sail with a downward component over the back end of the sail. The blunt trailing edge leads to a separation at the back end as shown in Fig. 9 for both the computation and wind tunnel flow visualization using a liquid crystal coating, which reacts to changes in shear in the boundary layer. Shown in Fig. 10 are streamlines on the hull around the sail. Again no traditional necklace vortex is generated, but there is significant flow turning. Streamlines behind the sail again have an outward component due to the secondary flow created by this sail. Comparisons of the computed axial velocity with that measured in the LCC are shown in Fig. 11. The bulge out of the flow from the hull is weaker than seen for the first sail due to a weaker vortex generated around the sail. This vortex bulge is considerably outboard from the centerline also. With this weaker vortex the k-ε model does a good job of predicting the flow, better than it did for the first sail. The q-ω model again produces a stronger vortex than the k-ε model, but again is in reasonable agreement with the data.
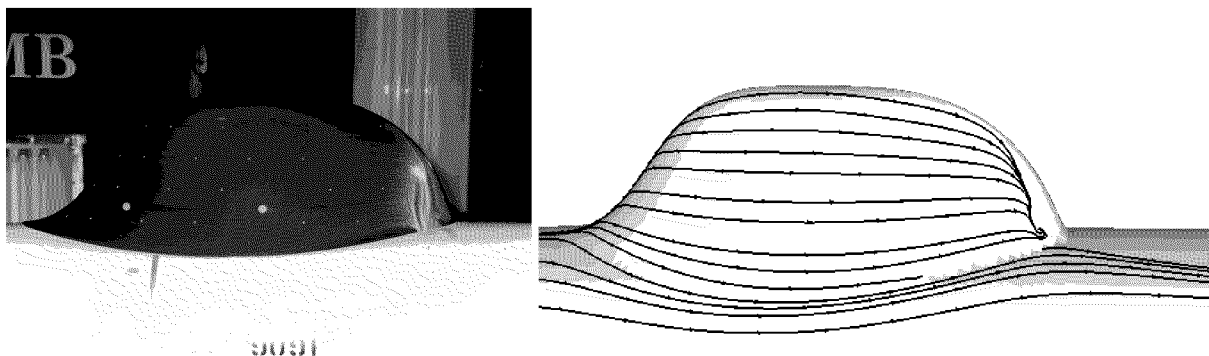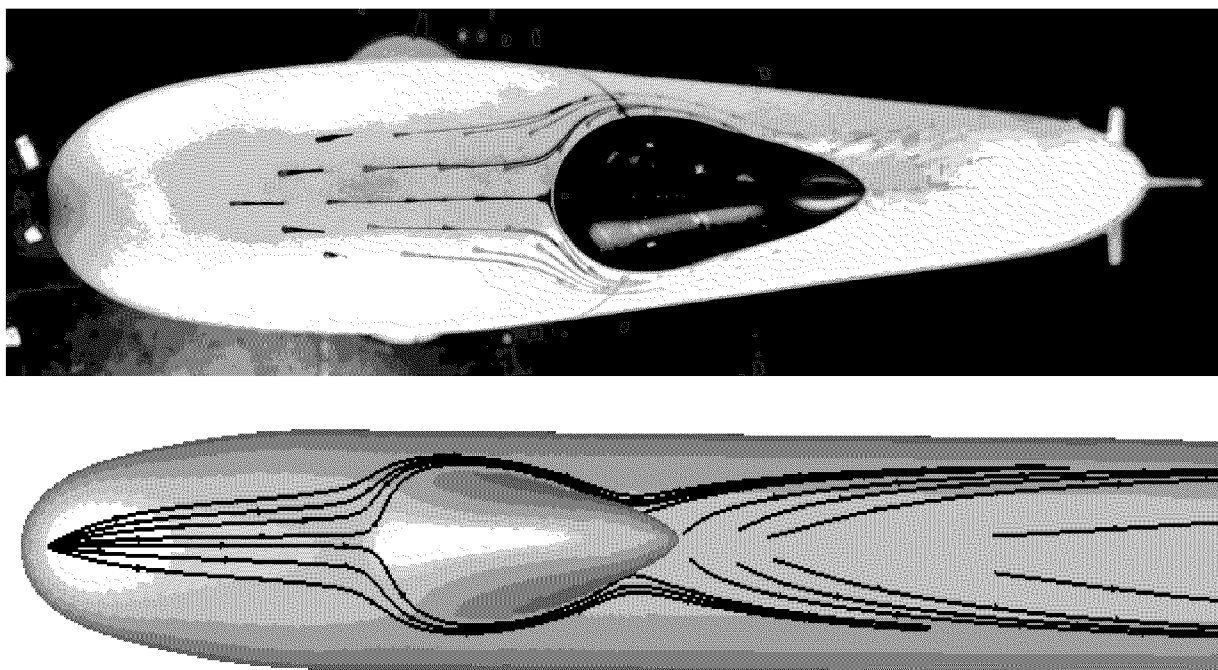
Fig. 9  Surface streamlines on the 2$^{nd}$ sail shape.
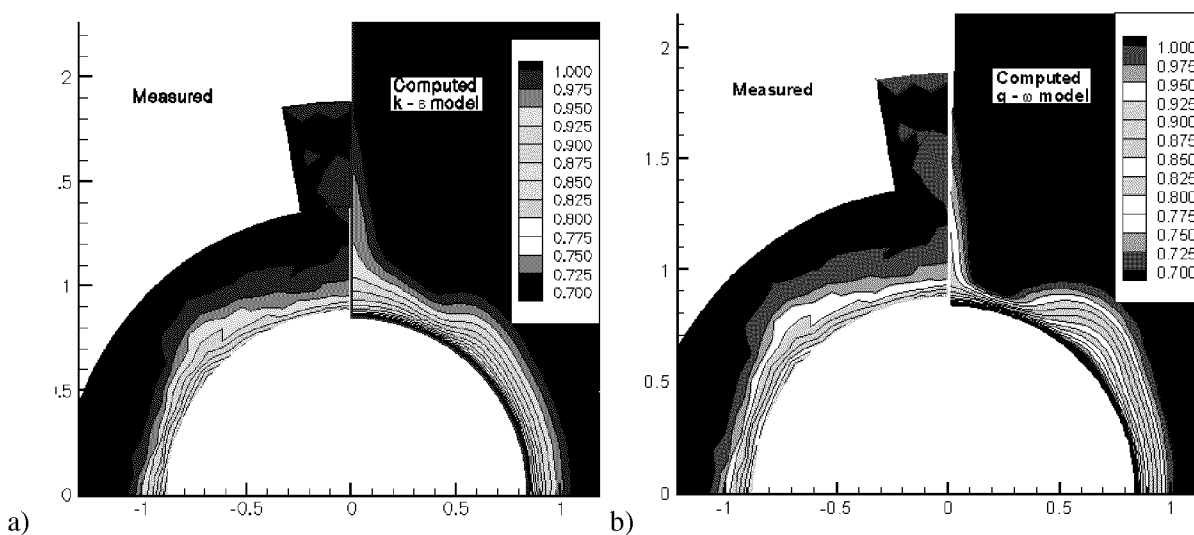


Fig. 10  Hull streamlines around the second sail.



Fig. 11  Computed and measured axial velocity contours at X/L = 0.825; a) k-ε model; b) q-ω model.

## Redesign Effort

The above computations demonstrate that RANS calculations can predict the significant flow features due to these sail shapes as well as differences between them. Additionally, the computations are able to predict the relative difference in drag between the two shapes. The second sail creates more drag than the first sail, possibly due to the blunter stern and leading edge. The first sail has more internal volume, but produces stronger secondary flow, which will convect downstream into the propeller. To try to combine some of the benefits of both a redesign effort is pursued to see if the shape can be improved. The first sail is chosen as the starting point due to its greater volume and less drag. To minimize changes to the sail only the back end is changed in effect retaining the drag reducing properties of the first sail. Also, it is believed that the blunter stern of the second sail helps reduce the strength of the secondary flow. Three different modifications are shown here. These changes involve increasing the trailing edge steepness of the spine. Efforts are also made to maintain the same length so as not to lose internal volume. A side view of these three shapes is shown in Fig. 12 and referred to as Mod-A, Mod-B, and Mod-C. Surface streamlines for the three shapes as well as axial velocity contours as compared to the original sail are shown in Fig. 13. Mod-A is the smallest change and provides a small knuckle at the back end. This knuckle creates a blunter trailing edge to the sail which leads to a slight flow separation there with a 0.8% increase in drag over the original sail. However, this small change produces a significantly weaker vortex as evidenced by the much smoother axial velocity contours. This smoother flow entering the propeller is very desirable. Mod-B is a very blunt stern with significant flow separation at the stern, which increases the drag 3.2% over the original sail and leads to an even stronger vortex than the original sail. Obviously, this very blunt stern does not work with the streamlined shape of this sail. Mod-C has a higher profile than the other modifications with some bluntness toward the back end. This sail shape also reduces the secondary flow over the original shape and provides an axial velocity field similar to Mod-A. It larger size leads to a 1.2% drag increase over the original sail. This effort has demonstrated two alternatives to the original sail shape, which provide significantly smoother flow into the propeller with a modest drag penalty. Subsequently, Mod-A was chosen, based largely on these computations, and efforts proceeded to build and test a 1/20 scale model at the LCC. This new sail, designated AS98, was then built and tested on the Large Scale Vehicle (1/4 scale) at the NSWCCD Acoustic Research Detachment in Bayview Idaho, Fig. 14.
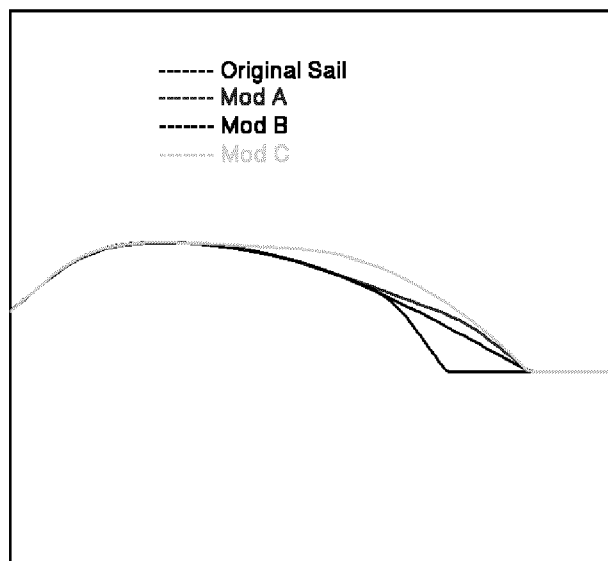


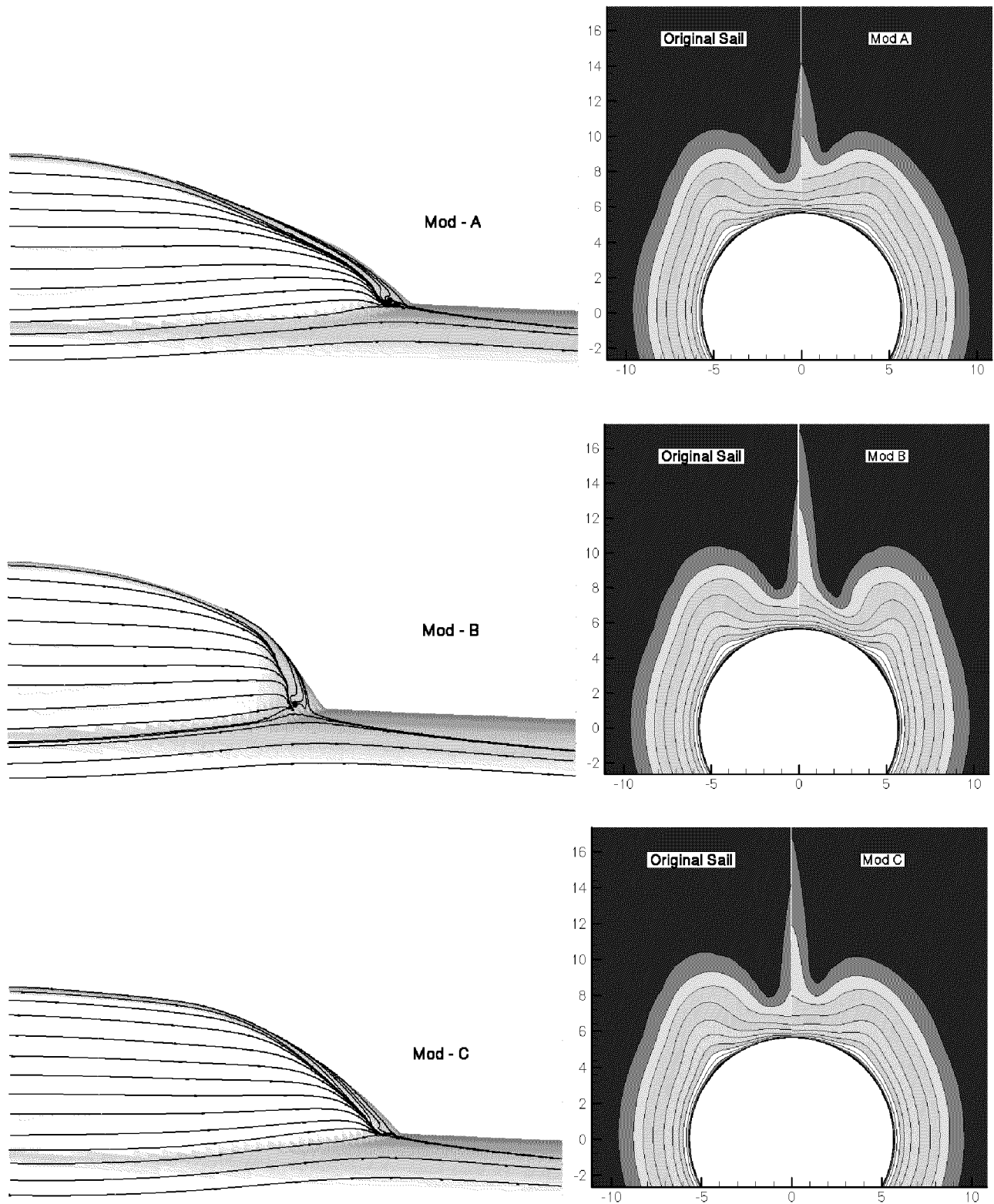Fig. 12 Side view of modified sail shapes.

Fig. 13 Surface streamlines and axial velocity contours for the redesigned sail shapes.

Fig. 14 Advanced Sail installed on the Large Scale Vehicle, from Dozier et al [1].

## Summary

Over the last decade there has been increased emphasis on the use of computational tools to evaluate submarine flows and guide their design. In particular, with the advent of parallel computational capabilities, viscous RANS simulations have seen a larger role in predicting these flow fields. The shift to a more computational based design and analysis approach leads to the possibility of better designs in a shorter amount of time. Such computations allow for the rank ordering of designs as well as providing the entire flow field, which can lead to better understanding of the flow physics. The current effort demonstrates the use of a RANS code in the design of an "Advanced Sail" for a submarine. The code is validated on similar sail shapes by comparing with experimentally obtained data from a wind tunnel and a water channel. This data comparison includes flow visualization, axial velocity and surface pressures. The agreement demonstrates that RANS codes can be used to provide the significant hydrodynamics associated with these sail shapes. Modifications to a sail are evaluated computationally providing drag differences as well as the secondary flow downstream of the sail. This allowed for the development of an improved shape, which was subsequently built and tested at 1/4 scale with plans for future implementation on the Virginia Class of submarines. Such computations provide a cost effective way to evaluate various shapes, that may improve a design, without having to build and test them. In this way computations will eventually reduce many design oriented tests, such as the series tests of old, which will be replaced with more comprehensive tests of the final design to fully evaluate and understand it.

## Acknowledgment

## References

[1] Dozier, D., Stout, M., and Zoccola, M., "Advanced Sail Development," *Wavelengths, An Employee Digest of Events and Information*, Carderock Division, Naval Surface Warfare Center, pp. 15 – 17, June, 2001.

[2] Gorski, J. J., "Marine Vortices and Their Computation," *Proc. NATO RTO Applied Vehicle Technology Panel Symposium on Advanced Flow Management*, Loen, Norway, May, 2001.

[3] Gorski, J. J., Coleman, R. M., and Haussling, H. J., "Computation of Incompressible Flow Around the DARPA SUBOFF Bodies," David Taylor Research Center Report, DTRC – 90/016, 1990.

[4] Liu, H-L. and Huang, T. T., "Summary of DARPA Suboff Experimental Program Data," NSWC Report, CRDKNSWC/HD – 1298 – 11, 1998.

[5] Atkins, D. J., "The Application of Computational Fluid Dynamics to the Hydrodynamic Design of Submarines," *Proc. Warship '99, Naval Submarines 6*, London, 1999.

[6] Gorski, J. J. "Drag Calculations of Unappended Bodies of Revolution," CRDKNSWC/HD-1362-07, May 1998.

[7] Taylor, L. K. and D. L. Whitfield, "Unsteady Three-Dimensional Incompressible Euler and Navier-Stokes Solver for Stationary and Dynamic Grids," AIAA Paper No. 91-1650, June 1991.

[8] Taylor, L. K., A. Arabshahi, and D. L. Whitfield, "Unsteady Three-Dimensional Incompressible Navier-Stokes Computations for a Prolate Spheroid Undergoing Time-Dependent Maneuvers," AIAA Paper No. 95-0313, Jan. 1995.

[9] Chorin, A. J., "A Numerical Method for Solving Incompressible Viscous Flow Problems," *Journal of Computational Physics*, Vol. 2, pp. 12-26, 1967.

[10] Van Leer, B., J. L. Thomas, P. L. Roe, and R. W. Newsome, "A Comparison of Numerical Flux Formulas for the Euler and Navier-Stokes Equations," AIAA Paper No. 87-1104-CP, June 1987.

[11] Whitfield, D. L. and L. K. Taylor, "Discretized Newton-Relaxation Solution of High Resolution Flux-Difference Split Schemes," AIAA Paper No. 91-1539, June 1991.

[12] Sheng, C., L. Taylor, and D. Whitfield, "Multiblock Multigrid Solution of Three-Dimensional Incompressible Turbulent Flows About Appended Submarine Configurations," AIAA Paper No. 95-0203, Jan. 1995.

[13] Taylor, L., K., et al., "Large-Scale Simulations for Maneuvering Submarines and Propulsors," AIAA Paper No. 98-2930, 1998.

[14] Liou, W. and T-H. Shih, "Transonic Turbulent Flow Predictions With New Two-Equation Turbulence Models," NASA Contractor Report 198444, Jan. 1996.

[15] Shih, T-H. and J. L. Lumley, "Kolmogorov Behavior of Near-Wall Turbulence and its Application in Turbulence Modeling," Comp. Fluid Dyn., Vol. 1, pp. 43 - 56, 1993.

[16] Coakley, T. J., "Turbulence Methods for the Compressible Navier-Stokes Equations,"AIAA Paper No. 83-1693, 1983.

[17] Walter, J. A. and V. C. Patel, "Measurements in Three-Dimensional Wake of a Surface-Mounted Winglike Symmetrical Ellipsoid," *Exp. Thermal Fluid Science*, Vol. 13, pp. 266 – 291, 1996.

[18] Gorski, J. J., "Present State of Numerical Ship Hydrodynamics and Validation Experiments," *Proc. OMAE'01, 20th Int. Conf. Offshore Mech. Arctic Eng.*, Rio de Janeiro, Brazil, OMAE01/OFT – 1350, June, 2001.

*Paper #33*
Discussor's name M. Bernard
Author J. J. Gorski

Q: Is it possible to take into account the free surface in your RANS calculations around submarines (sometimes, submarines are near the free surface, even if they are totally submerged)?

A: We are doing both linearized and non-linear free surface calculations with this same code for surface ships.


Discussor's name K. Orlik-Rukemann
Author J. J. Gorski

Q: 1. Are your calculations mainly applicable to the static case?
   2. Are maneuvering dynamics of submarines of much interest?

A: 1. Yes, static only
   2. Yes, it may be, especially for extreme cases.